

# NANO LETTERS

## Metalloporphyrin Nanotube Fabrication Using Peptide Nanotubes as Templates

Hiroshi Matsui<sup>\*,†</sup> and Robert MacCuspie<sup>‡</sup>

*Department of Chemistry at Hunter College, The City University of New York, New York, New York 10021, and Department of Chemistry, University of Central Florida, Orlando, Florida 32816*

*Received August 20, 2001; Revised Manuscript Received September 27, 2001*

### ABSTRACT

Protoporphyrin IX Zn(II) has been demonstrated to form metalloporphyrin coatings on peptide nanotubes via hydrogen bonds and produce metalloporphyrin nanotubes. This diacid metalloporphyrin was stabilized on the peptide nanotube surfaces with two types of hydrogen bonds, intermolecular hydrogen bond between the carboxylic acid of metalloporphyrins and the amide of peptide nanotube and intermolecular hydrogen bond between the carboxylic acids of neighboring metalloporphyrins. Since previous study indicates that the peptide nanotubes can potentially be assembled as arrays, the applications of metalloporphyrin nanotubes to nanoscale chemical sensors or photonics may be possible.

### Introduction

Nanoscale nanotube arrays have been fabricated and proposed to apply to the next generation of magnetic recording media,<sup>1,2</sup> photovoltaic solar cells,<sup>3–5</sup> field emission,<sup>6–8</sup> and chemical sensors<sup>9–11</sup> since the array configurations produce very large surface-to-volume ratio with the high nanotube-packing density. In the fields of chemical sensors and photonics, porphyrin has been extensively studied because porphyrins are highly efficient in electron and energy transfers.<sup>12–14</sup> Porphyrins have also been demonstrated as excellent catalysts for oxidations.<sup>15,16</sup> The difficulty is the immobilization of porphyrins on surfaces with the large surface areas. One approach for porphyrin sensor fabrication is the immobilization of porphyrins via the self-assembled

monolayers (SAMs) on surfaces.<sup>17–20</sup> For example, porphyrin SAMs were immobilized on membrane-coated PVC films for a flow-through chemiluminescence sensor.<sup>21</sup>

While the SAM approach is two-dimensional in geometry, a three-dimensional approach such as array assemblies will increase surface areas, which will also increase sensitivity for sensor devices. If porphyrins can be assembled in high-density arrays, those structures may be applied to ultra sensitive chemical sensors or photonic devices. While fabrications of molecular scale porphyrin arrays have been very active,<sup>22–30</sup> our interest is to produce nanotube-based three-dimensional porphyrin arrays in large surface areas.

In this study, metalloporphyrin nanotubes were fabricated by using peptide nanotubes as templates. The peptide nanotubes were self-assembled from bis(*N*-α-amido-glycylglycine)-1,7-heptane dicarboxylate (Figure 1), a peptide molecule that forms crystalline tubular structures in a diameter range of 20 nm to 1 μm in a pH 6 solution.<sup>31,32</sup>

\* To whom correspondence should be addressed. E-mail: hiroshi.matsui@hunter.cuny.edu.

† The City University of New York.

‡ University of Central Florida.

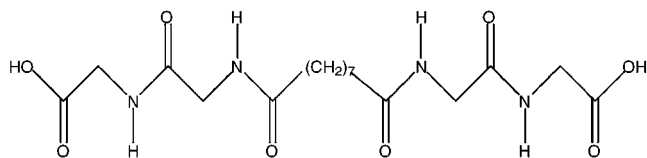


**Figure 1.** Chemical structure of the peptide molecule in order to assemble peptide nanotubes.

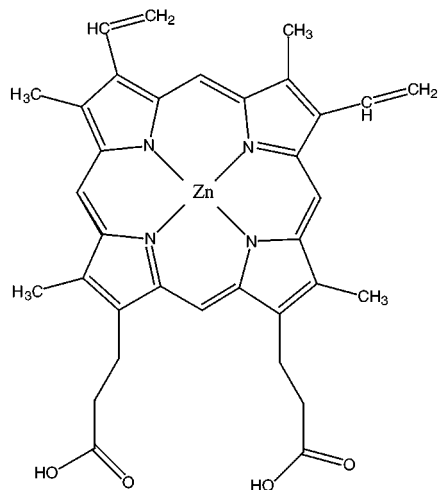


**Figure 2.** Chemical structure of diacid metalloporphyrin, protoporphyrin IX Zn(II).

The peptide nanotubes were used as templates for two reasons. First, using their free amide groups,<sup>31</sup> the peptide nanotubes can intercalate various molecules such as carboxylic acid-capped quantum dots<sup>33</sup> and proteins<sup>34</sup> via hydrogen bonds. Since protoporphyrin IX Zn(II) possesses two carboxylic acid groups (Figure 2), this metalloporphyrin is expected to coat the peptide nanotubes via hydrogen bonds. Second, the template peptide nanotubes showed potential to form arrays on carboxylic acid SAM/Au surfaces.<sup>35</sup> If metalloporphyrins can coat the peptide nanotubes to form metalloporphyrin nanotubes, these nanotubes may be able to assemble array structures on surfaces for future sensor applications.

In this report, we examined protoporphyrin IX Zn(II) to coat the peptide nanotubes. The coated metalloporphyrin nanotubes were also studied by FTIR microscopy to analyze the binding conformations between metalloporphyrins and peptide nanotubes. Previously, porphyrins have been immobilized on molecular sieves<sup>36,37</sup> or aggregated to form tubular structures with surfactants.<sup>38</sup> Recently, Ni nanotubes were coated by a luminescent porphyrin as a marker to probe dynamics of Ni nanotubes in magnetic fields.<sup>39</sup> To our knowledge, this study is the first example to fabricate metalloporphyrin nanotubes using peptide nanotubes as templates. This outcome may also be applied to fabricate nanoscale devices using metalloporphyrin–ligand interactions (i.e., site-specific assemblies of metalloporphyrin nanotubes on patterned ligand SAMs), while a similar assembly method was recently demonstrated for electronic applications using protein–protein interactions.<sup>40</sup> Investiga-

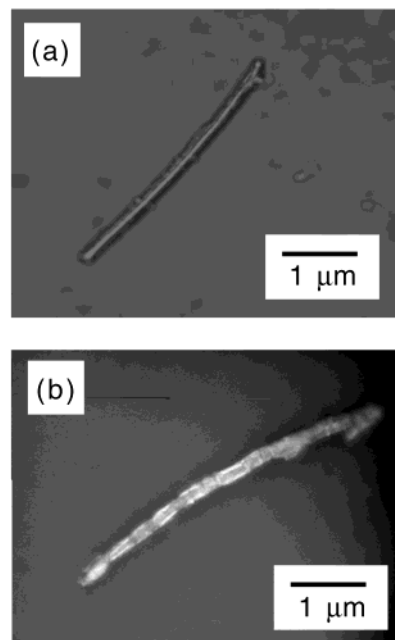


**Figure 3.** Light micrographs of (a) the neat peptide nanotube (b) the metalloporphyrin-coated peptide nanotube.

tions of the metalloporphyrin array assemblies and the sensing performances are underway.

## Experimental Section

The method to synthesize the peptide nanotubes has been reported previously.<sup>31</sup> To ensure a high degree of purity, the nanotubes were rinsed five times with deionized water using a centrifuge. Meanwhile, protoporphyrin IX Zn(II) (Aldrich Chemical Co., Figure 2) was dissolved in a solvent of ethanol and DMF (4:1 V/V). Then, 200  $\mu$ L of the peptide nanotube solution, containing  $2 \times 10^{-4}$  M of the peptide monomer, was loaded into 200  $\mu$ L of the  $2 \times 10^{-4}$  M Zn metalloporphyrin solution to produce metalloporphyrin monolayers on the nanotubes. This solution was allowed to stand for 72 h at room temperature for the metalloporphyrin immobilization on the peptide nanotubes.

In preparation for FTIR microscopic analysis, the Zn metalloporphyrin-coated nanotubes were centrifuged until aggregates were formed. After excess solvent was removed, the aggregates were allowed to dry in air for 24 h on a diamond anvil microcell for FTIR microscopy.

## Results and Discussion

A light micrograph of the neat peptide nanotube shows that the nanotube was dark (Figure 3a). However, when the peptide nanotube was mixed with the metalloporphyrin solution, the nanotube appeared brighter (Figure 3b). This observation is due to the absorption of visible light with the metalloporphyrins and indicates that the metalloporphyrins were adsorbed on the peptide nanotube surfaces. The distribution of metalloporphyrins was uniform on the peptide

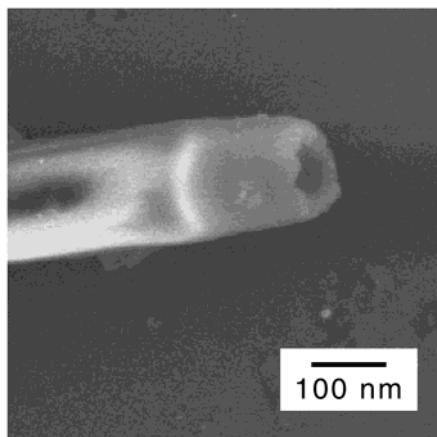


**Figure 4.** A scanning electron micrograph (SEM) of the metalloporphyrin-coated peptide nanotube.

nanotubes in Figure 3b, and the metalloporphyrin-coated nanotubes became brighter when concentrations of metalloporphyrins were increased. A scanning electron micrograph (SEM) of the metalloporphyrin-coated nanotube is shown in Figure 4. A hollow structure of the template nanotube was preserved even after the metalloporphyrins were coated on the nanotube surfaces.

To probe binding conformations between metalloporphyrins and peptide nanotubes, vibrations of the metalloporphyrins on the peptide nanotubes were characterized using an FTIR microscope. A Raman microscope was also applied to study the metalloporphyrin-coated peptide nanotubes, but the signal-to-noise ratios of the Raman spectra were too low to characterize their vibrational modes due to their low Raman cross sections. The FTIR spectra of metalloporphyrin-coated nanotubes, neat metalloporphyrin and neat peptide nanotubes are shown in Figure 5. Most of the peaks in the neat metalloporphyrin spectrum (Figure 5b) appear in the metalloporphyrin-coated nanotube spectrum (Figure 5a), whereas some major peaks in the neat peptide nanotube spectrum (Figure 5c) were absent in the metalloporphyrin-coated nanotube spectrum. For example, peaks at 1107 and 1265  $\text{cm}^{-1}$  in the neat peptide nanotube spectrum were not observed in the metalloporphyrin coated nanotube spectrum. This observation indicates that most of the IR was absorbed by the metalloporphyrin coatings on the peptide nanotubes. While it is possible that peaks from the peptide nanotubes may still be present in the metalloporphyrin-coated nanotube spectrum, the signal of the peptide nanotubes has been attenuated to a level that the signal-to-noise ratio is insufficient to conclusively confirm the presence of those met-

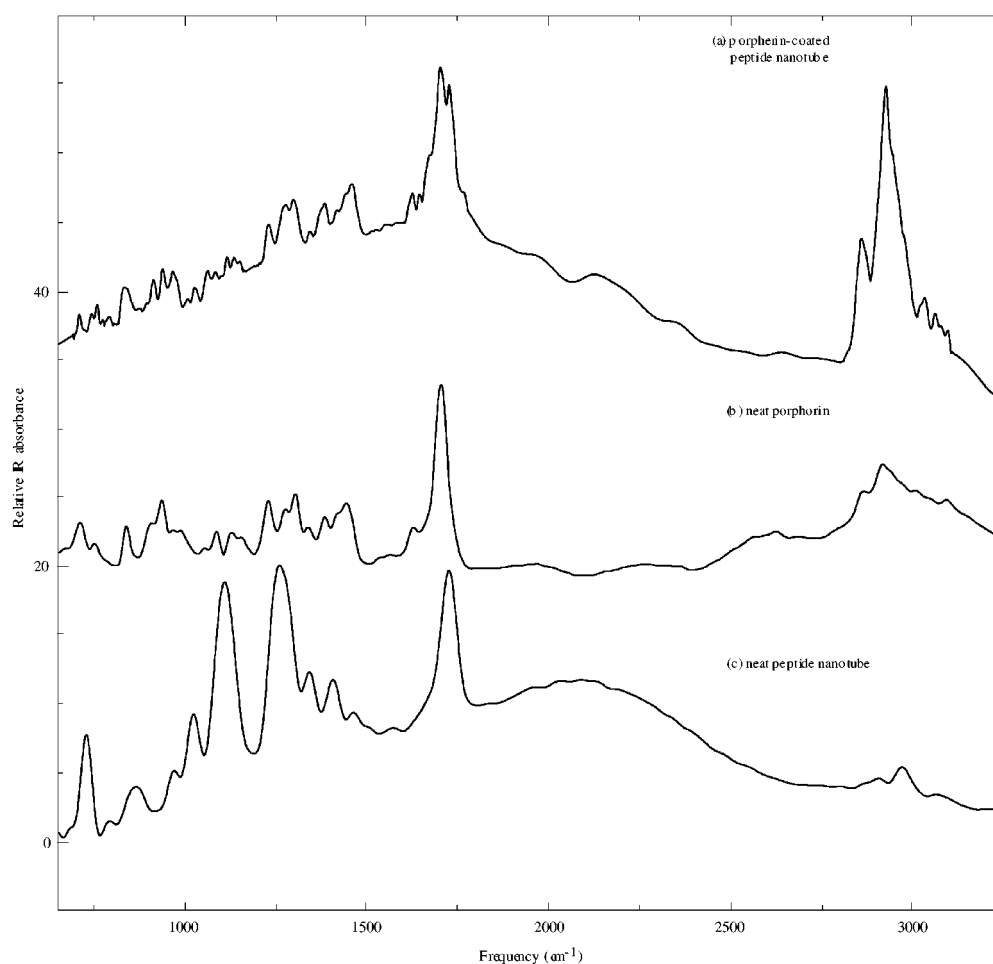


**Figure 5.** FTIR microscopic spectra of (a) the metalloporphyrin-coated peptide nanotube, (b) the neat metalloporphyrin, and (c) the neat peptide nanotube.

alloporphyrin peaks. Comparison of the metalloporphyrin spectrum (Figure 5b) and the metalloporphyrin-coated nanotube spectrum (Figure 5a) reveals several peaks in common. Peaks at 834, 932, 980, 1118, 1224, 1270, 1380, 1450, and 1624  $\text{cm}^{-1}$  are all present in both spectra. This observation confirms that the metalloporphyrins were adsorbed on the peptide nanotubes.

The carboxylic acid peaks between 1700 and 1800  $\text{cm}^{-1}$  in Figure 5 are of the highest interests because frequencies of carbonyl ( $\text{C}=\text{O}$ ) stretches of the metalloporphyrins on the nanotubes should contain information for hydrogen bonding conformations between the  $\text{COOH}$  of metalloporphyrins and the peptide nanotubes. The 1704  $\text{cm}^{-1}$  peak was observed in the metalloporphyrin-coated nanotube spectrum (Figure 5a) and the neat metalloporphyrin spectrum (Figure 5b). Therefore, the 1704  $\text{cm}^{-1}$  peak in the metalloporphyrin-coated nanotube spectrum originated from the carbonyl stretch of the metalloporphyrin's carboxylic acid groups. The 1704  $\text{cm}^{-1}$  peak is red-shifted in comparison with the carbonyl stretch in gas-phase carboxylic acid, 1772  $\text{cm}^{-1}$ ,<sup>41</sup> because metalloporphyrins are dimerized by forming a pair of hydrogen bonds between the carboxylic acid groups of each molecule in the condensed phase.<sup>42</sup> This spectroscopic observation indicates that metalloporphyrins on the peptide nanotubes form intermolecular hydrogen bonds between carboxylic acid groups. Another carbonyl mode observed at a 1719  $\text{cm}^{-1}$  was assigned as a hydrogen bond between the carbonyl group of metalloporphyrins and the amide group of peptide nanotubes. While amide frequency shifts of the peptide nanotubes could not be confirmed due to their weak IR absorbances, previous results indicate that the amide groups are the only free functional groups in the peptide nanotubes to bind carboxylic acid groups of coating materials.<sup>33,34,43</sup> Therefore, it is likely that the carbonyl group of metalloporphyrins binds the amide group of peptide nanotubes for the immobilization. Because the 1719  $\text{cm}^{-1}$  is blue-shifted in comparison with the 1704  $\text{cm}^{-1}$ , the hydrogen bonds between metalloporphyrins and peptide nanotubes seem to be weaker than the acid–acid dimer hydrogen bonds between metalloporphyrins. These spectroscopic results suggest that one of carboxylic acid groups in diacid metalloporphyrins binds the peptide nanotubes and the other carboxylic acid group in diacid metalloporphyrins binds neighboring diacid metalloporphyrins. This hydrogen bonding conformation is illustrated in Figure 6.

This type of porphyrin-binding conformation on surfaces has been observed previously.<sup>18</sup> Recently, study of diacid metalloporphyrin SAMs on Au surfaces showed that the diacid metalloporphyrin SAMs were immobilized with two interactions, acid–acid dimer hydrogen bonds between diacid metalloporphyrins and electrostatic interactions between carbonyl groups of diacid metalloporphyrins and Au.<sup>44</sup> This study indicates that one of carboxylic acids in diacid metalloporphyrins binds Au and the other carboxylic acid group in diacid metalloporphyrins binds neighboring diacid metalloporphyrins, which is similar to our proposed binding conformation. These interactions were reported to add stability of the diacid metalloporphyrin SAMs on Au

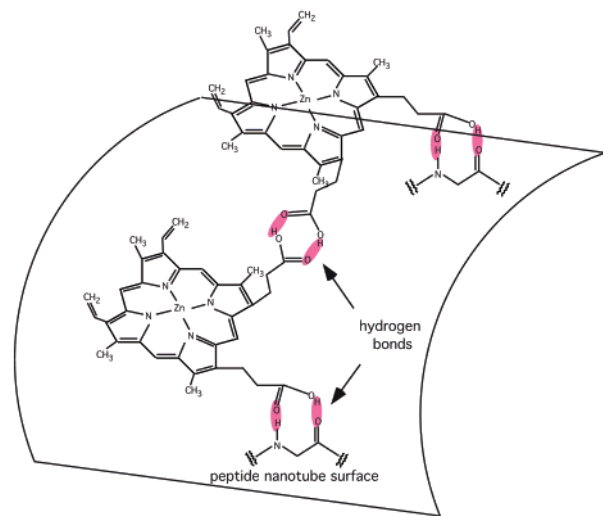


**Figure 6.** Proposed binding conformation of the metalloporphyrin-coated peptide nanotube.

surfaces.<sup>44</sup> In our system, the two interactions, diacid metalloporphyrin–peptide nanotube hydrogen bonds and metalloporphyrin–metalloporphyrin hydrogen bonds, may also provide excellent stability in the metalloporphyrin attachment on the peptide nanotube surfaces. This stability may reflect the observation that the metalloporphyrin-coatings were maintained even after extensive washing processes.

While we understand that determination of the metalloporphyrin orientation on the peptide nanotube surfaces is difficult since the surfaces are not flat, vibrational frequencies of metalloporphyrin ring and  $\text{CH}_2$  chains suggest that metalloporphyrin molecules were tilted with respect to the nanotube surfaces. The CN stretching mode of the metalloporphyrin ring at 1385  $\text{cm}^{-1}$  decreases by 6  $\text{cm}^{-1}$  in the metalloporphyrin-coated nanotube spectrum, Figure 5a. This frequency shift indicates that the metalloporphyrin molecules were tilted on the nanotube surfaces.<sup>45</sup> Blue shifts of the metalloporphyrin  $\text{CH}_2$  symmetric (2860  $\text{cm}^{-1}$ ) and antisymmetric (2923  $\text{cm}^{-1}$ ) modes on the nanotubes, 9 and 12  $\text{cm}^{-1}$  upshifts compared with neat metalloporphyrin, also suggest the tilting conformation of metalloporphyrin molecules.<sup>45</sup>

Here we demonstrated that protoporphyrin IX Zn(II) forms the metalloporphyrin coatings on peptide nanotubes via hydrogen bonds and produces metalloporphyrin nanotubes. Spectroscopic analysis of the metalloporphyrin-coated nanotubes indicates that one of the carboxylic acid groups of the diacid metalloporphyrins binds to the amide group of peptide nanotubes, while the other carboxylic acid group of the diacid metalloporphyrins binds to the carboxylic acid group of neighboring metalloporphyrins. Since the peptide nanotubes can potentially be assembled as arrays with large surface areas,<sup>35</sup> the application of metalloporphyrin nanotubes to nanoscale chemical sensors or photonics may be possible.

**Acknowledgment.** R.M. acknowledges Professor B. Fookes for assistance with FTIR microscopy. This work was

supported by the NER program of the NSF and the Office of Basic Energy Sciences of the DOE.

## References

- (1) Savas, T. A.; Farhoud, M.; Hwang, M.; Smith, H. I.; Ross, C. A. *J. Appl. Phys.* **1999**, *85*, 6160.
- (2) Abraham, M. C.; Schmidt, H.; Savas, T. A.; Smith, H. I.; Ross, C. A.; Ram, R. J. *J. Appl. Phys.* **2001**, *89*, 5667.
- (3) Karpov, V. G.; Rich, G.; Subashiev, A. V.; Dorer, G. *J. Appl. Phys.* **2001**, *89*, 4975.
- (4) Bleijs, J. A. M.; Gow, J. A. *Electron Lett.* **2000**, *37*, 5.
- (5) Musca, D. A.; Dell, J. M.; Faraone, L.; Baijaj, J.; Pepper, T.; Spariosu, K.; Blackwell, J.; Bruce, C. J. *Electron Mater.* **1999**, *28*, 617.
- (6) Davydov, D. N.; Sattari, P. A.; AlMawlawi, D.; Osika, A.; Haslett, T. L.; Moskovits, M. *J. Appl. Phys.* **1999**, *86*, 3983.
- (7) de Heer, W. A.; Chatelain, A.; Ugrte, D. *Science* **1995**, *270*, 1179.
- (8) Collins, P. G.; Zettl, A. *Phys. Rev. B* **1997**, *55*, 9391.
- (9) Kong, J.; Franklin, N.; Zhou, C.; Chapline, M.; Peng, S.; Cho, K.; Dai, H. *Science* **2000**, *287*, 622.
- (10) Collins, P.; Bradley, K.; Ishigami, M.; Zettl, A. *Science* **2000**, *287*, 1801.
- (11) Jhi, S.-H.; Louie, S. G.; Cohen, M. L. *Phys. Rev. Lett.* **2000**, *85*, 1710.
- (12) Imahori, H.; Norieda, H.; Yamada, H.; Noshimura, Y.; Yamazaki, I.; Sakata, Y.; Fukuzumi, S. *J. Am. Chem. Soc.* **2001**, *123*, 100.
- (13) Drain, C. D.; Nifiatis, F.; Vasenko, A.; Batteas, J. D. *Angew. Chem., Int. Ed. Engl.* **1998**, *37*, 2344.
- (14) Deviprasad, G. R.; D'Souza, F. *Chem. Commun.* **2000**, 1915.
- (15) Gonsalves, A. M. D. R.; Serra, A. C. *J. Mol. Catal. A—Chem.* **2001**, *168*, 25.
- (16) Huang, J. W.; Mei, W. J.; Liu, J.; Ji, L. N. *J. Mol. Catal. A—Chem.* **2001**, *170*, 261.
- (17) Kalyuzhny, G.; Vaskevich, A.; Ashkenasy, G.; Shanzer, A.; Rubinstein, I. *J. Phys. Chem. B* **2000**, *104*, 8238.
- (18) Zhang, Z. J.; Imae, T.; Sato, H.; Watanabe, A.; Ozaki, Y. *Langmuir* **2001**, *17*, 4564.
- (19) Offord, D. A.; Sachs, S. B.; Ennis, M. S.; Eberspacher, T. A.; Griffin, J. H.; Chidsey, C. E. D.; Collman, J. P. *J. Am. Chem. Soc.* **1998**, *120*, 4478.
- (20) Da Cruz, F.; Driaf, K.; Berthier, C.; Lameille, J. M.; Armand, F. *Thin Solid Films* **1999**, *349*, 155.
- (21) Kuniyoshi, A.; Hattai, K.; Suzuki, T.; Masuda, A.; Yamada, M. *Anal. Lett.* **1996**, *29*, 673.
- (22) Rakow, N. A.; Suslick, K. S. *Nature* **2000**, *406*, 710.
- (23) Drain, C. D.; Fischer, R.; Nolen, E.; Lehn, J.-M. *J. Chem. Soc., Chem. Commun.* **1993**, 243.
- (24) Araki, K.; Wagner, M. J.; Wrighton, M. S. *Langmuir* **1996**, *12*, 5393.
- (25) Brunink, J. A. J.; DiNatale, C.; Bungaro, F.; Davide, F. A. M.; D'Amico, A.; Paolesse, R.; Boschi, T.; Faccio, M.; Ferri, G. *Anal. Chim. Acta* **1996**, *325*, 53.
- (26) Slone, R. V.; Hupp, J. T. *Inorg. Chem.* **1997**, *36*, 5422.
- (27) Stang, P. J.; Fan, J.; Olenyuk, B. *Chem. Commun.* **1997**, 1453.
- (28) Redman, J. E.; Feeder, N.; Teat, S. J.; Sanders, J. K. M. *Inorg. Chem.* **2001**, *40*, 2486.
- (29) Yuan, H.; Thomas, L.; Woo, L. K. *Inorg. Chem.* **1996**, *35*, 2808.
- (30) Wilson, G. S.; Anderson, H. L. *Chem. Commun.* **1999**, 1539.
- (31) Matsui, H.; Gologan, B. *J. Phys. Chem. B* **2000**, *104*, 3383.
- (32) Kogiso, M.; Ohnishi, S.; Yase, K.; Masuda, M.; Shimizu, T. *Langmuir* **1998**, *14*, 4978.
- (33) Matsui, H.; Pan, S.; Douberly, G. E. J. *J. Phys. Chem. B* **2001**, *105*, 1683.
- (34) Douberly, G. E. J.; Pan, S.; Walters, D.; Matsui, H. *J. Phys. Chem. B* **2001**, *105*, 7612.
- (35) Matsui, H.; Gologan, B.; Pan, S.; Douberly, G. E., Jr. *Eur. Phys. J. D* **2001**, *16*, 403.
- (36) SungSuh, H. M.; Luan, Z. H.; Kevan, L. *J. Phys. Chem. B* **1997**, *101*, 10455.
- (37) Goldberg, I. *Chem-Eur. J.* **2000**, *6*, 3863.
- (38) Komatsu, T.; Yanagimoto, T.; Furubayashi, Y.; Wu, J.; Tsuchida, E. *Langmuir* **1999**, *15*, 4427.
- (39) Tanase, M.; Bauer, L. A.; Hultgren, A.; Silevitch, D. M.; Sun, L.; Reich, D. H.; Searson, P. C.; Meyer, G. J. *Nano Lett.* **2001**, *1*, 155.
- (40) Matsui, H.; Porrata, P.; Douberly, G. E. J. *Nano Lett.* **2001**, *1*, 461.
- (41) Yamamoto, M.; Iwai, Y.; Nakajima, T.; Arai, Y. *J. Phys. Chem. A* **1999**, *103*, 3525.
- (42) Lin-Vien, D.; Colthup, N. B.; Fateley, W. G.; Grasselli, J. G. *The Handbook of Infrared and Raman Characteristic Frequencies of Organic Molecules*; Academic Press: New York, 1991.
- (43) Matsui, H.; Pan, S.; Gologan, B.; Jonas, S. *J. Phys. Chem. B* **2000**, *104*, 9576.
- (44) Zhang, Z.; Imae, T. *Nano Lett.* **2001**, *1*, 241.
- (45) Zhang, Z.; Verma, A. L.; Yoneyama, M.; Nakashima, K.; Iriyama, K.; Ozaki, Y. *Langmuir* **1997**, *13*, 4422.

NL0156080